ELECTROCHEMICAL IMPEDANCE SPECTROSCOPY STUDY OF H_2O_2 INTERACTION WITH γ-FeOOH SINGLE-PHASE FILMS ON THE GOLD ELECTRODES

Dong Fu

Department of Chemistry, The University of Western Ontario, London, Ontario, Canada
N6A 5B7

1. Introduction

CANDU reactor is one of the three major commercial power reactor design used throughout the world. For the heat transport system (HTS) of a CANDU reactor, inside the reactor core is 2.5 wt% Nb alloy pressure tubes and connect carbon steel pipes outside the core.

Corrosion of these pipes under reactor operating conditions is a main concern for aging CANDU reactors. Steel corrosion releases metal ions into the coolant, which can precipitate along the circuit, potentially affecting the heat transfer efficiency of the system. Their neutron activation prior to precipitation can increase radioactivity levels outside the reactor core, and pose a safety problem during reactor shutdown and maintenance. Various measures have been taken to minimize these effects, such as coolant purification and filtration and the adoption of pH control to minimize solubility. Concern about steel corrosion is not limited to CANDU, but also to PWR (pressurized water reactor) and BWR (boiling water reactors), although these reactors use stainless steel.

The corrosion of steels is strongly affected by the presence of oxide films, which vary considerably in reactivity and solubility. Generally, corrosion studies have been limited to the low corrosion potential range where carbon steel in de-aerated water is typically poised. In this potential range, the surface oxide film is considered to be mainly magnetite, Fe_3O_4 [1], but more recent studies on the synergistic interaction of water radiolysis and carbon steel corrosion [2] suggest that H_2O_2, produced by radiolysis, can increase the corrosion potential to a range where Fe(III) oxides, such as Fe_2O_3 and FeOOH, may also form in addition to Fe_3O_4. These surface oxides may interact with water radiolysis products very differently, making it difficult to predict the effect of radiation on steel corrosion, since H_2O_2 may disproportionate on the oxide-covered surfaces ($H_2O_2 = 2O_2+H_2O$), as well as drive steel corrosion.

Our primary goal is to determine how radiolytic oxidants, such as H_2O_2, will interact with oxide-covered steel surfaces and what influence this will have in steel corrosion kinetics. However, oxide films formed on carbon steel are complex mixtures of several different iron oxides and oxyhydroxides, making the corrosion chemistry of steel notoriously complex. For example, lepidocrocite, γ-FeOOH, is a ubiquitous ferric oxyhydroxide that may enhance the rate of corrosion since it is suspected to act as an electron acceptor towards iron metal [3]. We have prepared single-phase oxide films on gold to facilitate electrochemical measurements on these oxides. By studying the behaviour of H_2O_2 on individual oxides/hydroxides we hope to be able to characterize the more complicated behaviour of carbon steel surfaces in the presence of radiolytically-decomposed water.

In this paper, we prepared single-phase γ-FeOOH on the gold electrode and characterized with electrochemical impedance spectroscopy (EIS). The H_2O_2 reaction with the oxide films was then followed by corrosion potential, E_{CORR}, and EIS measurements as a function of exposure time to H_2O_2. Ex situ Raman spectroscopy were used to characterize the oxides/hydroxides films.

2. Experimental

2.1. Electrochemical system

A standard three-electrode cell, consisting of a gold working electrode, a reference electrode and a counter electrode, was used for all experiments. The working electrode was a 6-mm (in diameter) gold disc(goodfellows), set in resin so that only the flat front face was exposed to the solution. Prior to deposit film, this electrode was manually polished with 600 and 800 grit silicon carbide papers, and polishing residue removed by sonication in an acetone/methanol mixture for 5 min. The reference electrode was a saturated calomel electrode (SCE) and the counter electrode was platinum mesh. All potential measurements were made with, and are quoted against, a saturated calomel reference electrode (SCE).

A Solartron model 1240 potentiostat and 1252 frequency response analyzer were used in all electrochemical measurements. Corrware^{TM} and Corrview software (supplied by Scribner and Associates) was used to control experiments and analyze data. Electrochemical Impedance Spectroscopy (EIS) was performed by applying a 10 mV sinusoidal potential waveform at an open circuit potential over the frequency range 10 kHz to 10^{-2} Hz.

2.2. γ-FeOOH film preparition

The γ-FeOOH films were prepared following our previous work [4]. The gold electrodes were directly immersed 20 mmol/dm^3 $Fe(NO_3)_3$ solution suspended vertically. The film deposition time in the oven was 24 h and the oven temperature ranged from 60°C. The electrodes were then removed from the solutions, rinsed with distilled water, and suspended in air to dry at ambient temperature for 24 h.

2.3. Solutions

Experiments were conducted at room temperature in Ar-purged 0.01 M borate ($Na_2B_4O_7$) with the pH adjusted to 10.6 with NaOH (unless otherwise stated). Solutions were prepared with water purified using a NANOpure Diamond UV ultrapure water system from Barnstead International to remove organic and inorganic impurities. Prepared in this manner, the water had a resistivity of 18.2 MΩ cm.

A hydrogen peroxide stock solution was prepared by adding an appropriate amount of concentrated H_2O_2 (3% in the weight percentage) to the electrolyte solution to bring the H_2O_2 concentration to a desired value in the range of 10^{-4} to 10^{-3} mol dm^{-3} (M).

2.4. Experimental procedure

The experimental procedure used to study the interaction of electrochemically grown oxide films with H_2O_2 is presented schematically in Fig. 1. The E_{CORR} of the oxide covered gold electrode was allowed to relax for ~60 min to a pseudo steady-state value (Step 1), and the electrode/solution interface characterized by EIS (Step 2). The reaction of the oxide films with H_2O_2 was initiated by adding H_2O_2 to the electrolyte solution, to bring the H_2O_2 concentration to desire. The progress of the reaction was monitored by measuring E_{CORR} (Step 3), and recording EIS spectra at various reaction times (Step 4).

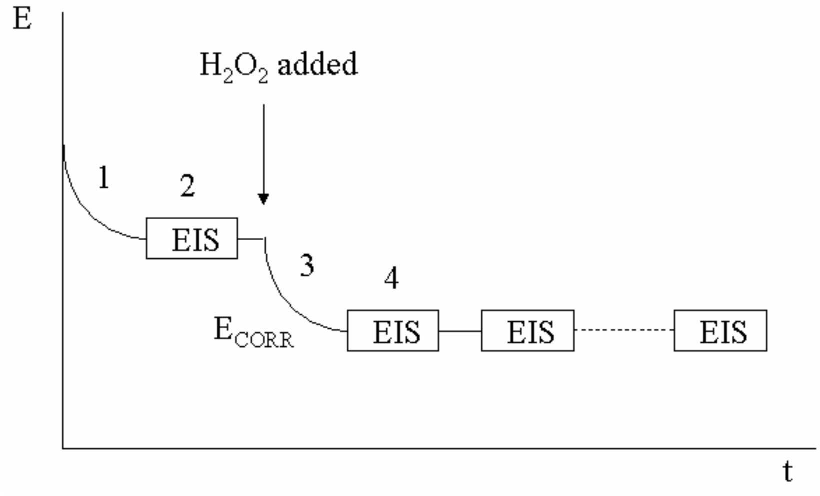

Fig. 1. Schematic of the experimental procedure used in this study.

2.5. Surface analysis

The Raman spectrum of the samples was measured using a Renishaw Ramascope Model 2000 (633 nm laser wavelength, approx. 2mW at the sample at 100% power, scan from 2000-120 cm^{-1}).

3. Results and discussion

3.1 Cyclic Voltammetry

Two voltammograms recorded at pH10.6 and room temperature are shown in Fig. 2. Scan from 0.2 V to –1.0 V and back to 0.2V.

For the γ-FeOOH films before exposed to H_2O_2, at cathodic scanning, current is very low in the range 0.2 ~ –0.5V. When potential passes the –0.5V, the current significantly increases, indicating reducing reactions occur. From equilibrium potentials and our prior to works [2, 5-7], the reducing reaction are γ-FeOOH to Fe_3O_4 and then Fe_3O_4 to Fe(II) species. At anodic scanning, the current significantly increases due to H_2 absorbed at electrode surface during cathodic scanning is reduced. The peak at –0.6V is assigned Fe(II) species oxidized, for example $Fe(OH)_2$ to Fe_3O_4. The peak at –0.4V is Fe_3O_4 oxidized to γ-FeOOH.

For the γ-FeOOH after exposed H_2O_2 12h, the voltammogram is slight different with before exposed to H_2O_2 indicating the γ-FeOOH film no significant changed. In the cathodic scanning, at –0.4V, an additional peak appears. Considering reducing reaction here, γ-FeOOH to Fe_3O_4 is assigned [8]. Because crystaline sizes of FeOOH (partially) decrease due to interaction with H_2O_2, the reducing reaction γ-FeOOH to Fe_3O_4 occurs early (partially). Detail discussion is in following sections.

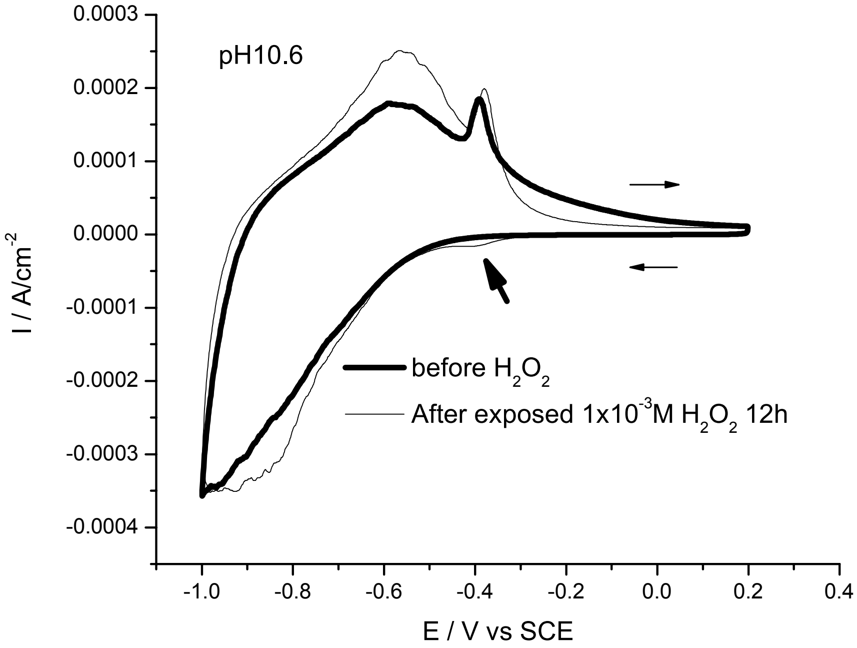

Fig. 2. Cyclic Votammetry of γ-FeOOH films on gold electrodes in pH 10.6 borate solutions. Scan rates 5mV/s. Scan after exposed in H2O2 γ-FeOOH film in Ar-purged fresh pH10.6 borate solutions.

3.2 Electrochemical impedance spectroscopy

The EIS spectrum of γ-FeOOH before expose to H_2O_2 can be fitted by one time constant (not shown). The resistance is ~1.8 MΩ and capacitance is ~20 µF. The resistance and capacitance are not change with time in pH 10.6 borate solution.

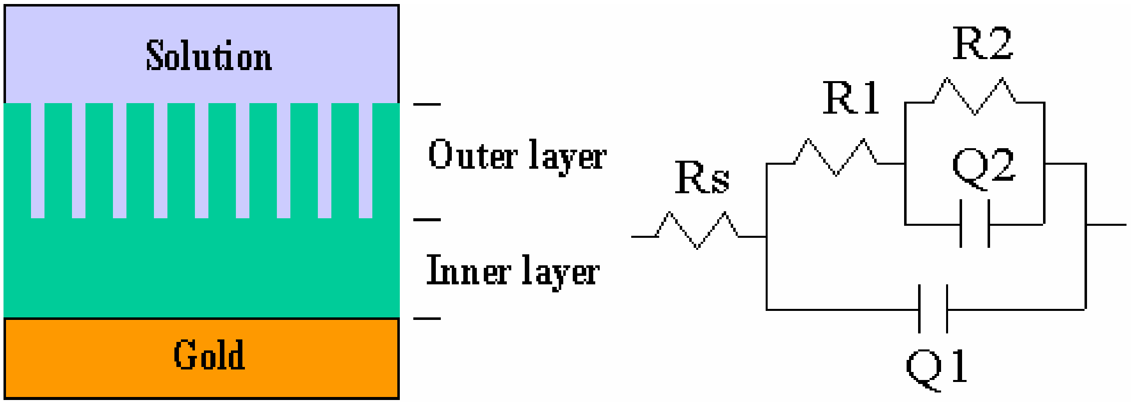

Fig. 3. The electrical equivalent circuit used in EIS analyses and Schematic representation of the γ-FeOOH film after exposed H_2O_2

Relaxing open circuit potential (OCP) of γ-FeOOH films in pH 10.6 borate solution, the OCP reaches steady-state after 1h. After adding H_2O_2 into the solution, the OCP immediately falls ~0.3V and the impedance falls several orders comparing with the film impedance before expose to H_2O_2, indicating the films break down and form more pores.

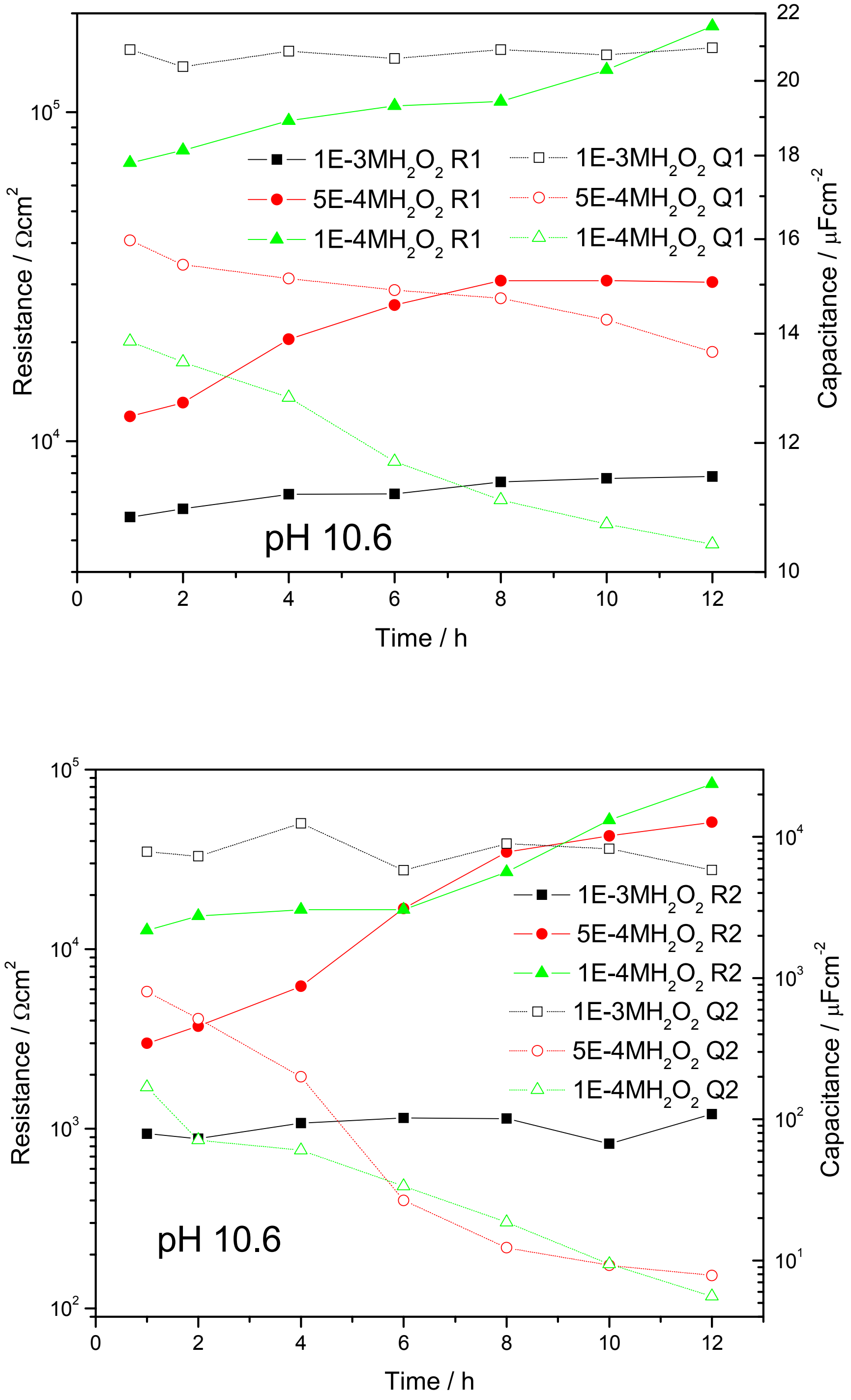

Fig. 4. Film resistances and capacitances obtained by fitting to the electric equivalent circuit in fig. 2.: (a) upper figure, the outer layer; and (b) lower figure, the inner layer.

EIS equivalent circuit as Fig. 3 shown has good fitting results for fitting γ-FeOOH films interaction with H_2O_2. It is consistent with film structure changing, namely, more pores formed in the films as shown at CV and OCP results.

In the equivalent circuit, Rs is bulk solution resistance. Q1 is capacitance of film outer layer. R1 is resistance of solution in the pores. R2 is resistance of film inner layer. Q2 is capacitance of film inner layer.

Fitting results of R1 and Q1 are shown in Fig. 4a, R2 and Q2 shown in Fig. 4b with various H_2O_2 concentration and reaction time. For the H_2O_2 concentration from 1×10^{-4}M rising to 1×10^{-3}M, the Q1 from ~11μF increases to ~21μF.

From equation $C = A\varepsilon_0\varepsilon/L$, where A is the geometrical surface area, ε_0 is the permissivity of free space. ε is the oxide film dielectric constant. L is the passive layer thickness. Q1 decreases following H_2O_2 concentration rising, indicating the outer layer thickness in higher concentration H_2O_2 is thinner than that in the lower H_2O_2 concentration. Similar trend can be found for Q2. Q2 decreases following H_2O_2 concentration rising, indicating the inner layer thickness in higher concentration H_2O_2 is thinner than that in the lower H_2O_2 concentration.

R1 increases following H_2O_2 concentrations rising, indicating the pore volumes increasing with rising H_2O_2 concentrations.

R2 decreases along with H_2O_2 concentration, indicating inner layer is thinner in higher H2O2 concentration, being consistent with Q2.

At lower concentration H_2O_2, 1×10^{-4}M, Q1 decreases with reaction time, indicating outer layer thickness increasing due to redeposition FeOOH on the surface [2]. Redeposition thickness is not too much because Q1 is just small change. Q2 is similar trend and increase significantly several orders indicating inner layer thickness increases much with reaction time. Redeposition effects is very significant in inner layer due to small pore volumes. In the small pore volume, soluble Fe(III) species cannot easily diffuse to the bulk solution. Therefore, when H_2O_2 is exhausted in the pore, the Fe(III) species (partially) redeposit on the inner layer.

R1 and R2 in 1×10^{-4}M H_2O_2 increase with time, indicating pore volumes reducing and inner layer thicker with time, due to redeposition, being consistent with Q2 capacitance results.

At H_2O_2 concentration 5×10^{-4} M, H_2O_2 effect is similar as 1×10^{-4} M. However, effect is enhanced due to higher H_2O_2 concentration.

At H_2O_2 concentration 1×10^{-3} M, R1, R2, Q1, Q2 just slightly change with reaction time. Because at higher H_2O_2 concentration, films form more pores and pore volumes are larger. Soluble Fe(III) species easily to diffuse into the bulk solution, therefore, redeposit effect is not significant.

3.3. Raman spectra

Fig. 5. shows Raman spectra of single-phase γ-FeOOH and after exposed to H_2O_2 1×10^{-3}M 12h. After exposed to H_2O_2 1×10^{-3}M 12h, all Raman peaks of the films are exactly match with single-phase γ-FeOOH peaks, suggesting the γ-FeOOH film composition does not change after interaction with H_2O_2. However, after exposed to H_2O_2, peak intensity slight reduces indicating film mircocrystalline change to smaller, which are consistent with analysis of CV and EIS.

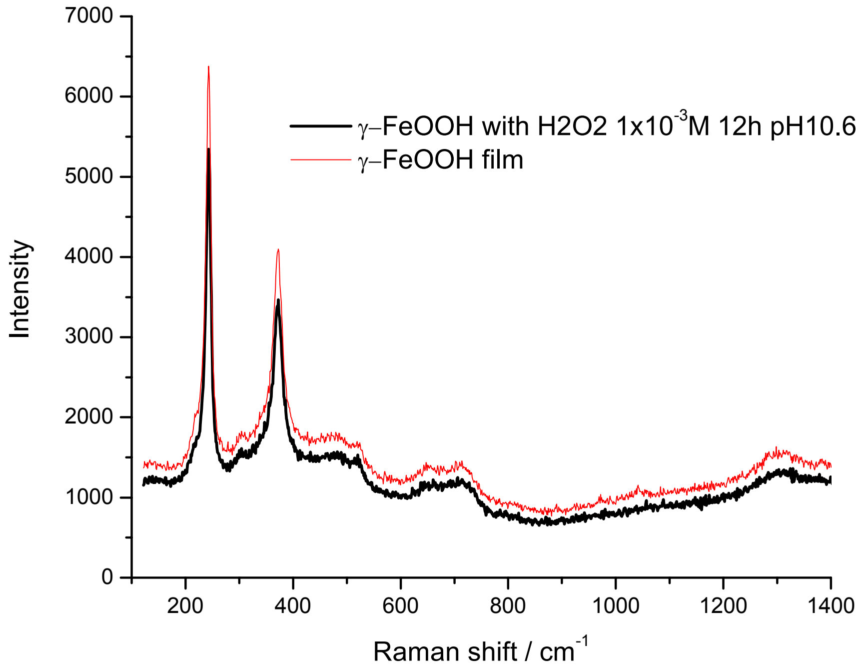

Fig. 5. Ex situ raman spectra of γ-FeOOH films: the upper spectrum is for a film not exposed to H_2O_2 while the lower spectrum is for a film exposed to 1×10^{-3}M H2O2.

4. Conclusion

CV, EIS and Raman spectra confirm the γ-FeOOH films composition does not appear to alter before or after exposed to H_2O_2. H_2O_2 interacts with FeOOH films resulting film break down and/or more pores formed. Furthermore, the γ-FeOOH films form two layers, porous outer layer and inner layer. The pores formed at lower concentration H_2O_2 have small volume. FeOOH redeposition occurs and makes pore volumes reduce, therefore, thickening inner layers and recover the films. Higher H_2O_2 concentration makes FeOOH films to form larger volume pores and redeposition does not significantly appear.

Acknowledgements

This work was performed under the Industrial Research Chair Program on Radiation Induced Processes in Nuclear Reactor Environments, funded by Canadian Natural Science and Engineering Research Council (NSERC) and Atomic Energy Canada Ltd. (AECL).

References:

[1] V. Malinovschi, C. Ducu, N. Aldea, M. Fulger, J. Nucl. Mater. 352 (2006) 107.
[2] X. Zhang, W. Xu, D.W. Shoesmith and J.C. Wren, Corros. Sci., 49 (2007) 4553.
[3] H. Antony, S. Peulon, L. Legr and A. Chausse´, Electrochim. Acta 50 (2004) 1015.
[4] D. Fu and J. C. Wren J. Nucl. Mater. 374 (2008) 116.

[5] M. Buchler, P. Schmuki, H. Bohni, J. Electrochem. Soc. 145 (1998) 609–614.
[6] M. Buchler, P. Schmuki, H. Bohni, J. Electrochem. Soc. 144 (1997) 2307–2312.
[7] A. Hugot–LeGo., J. Flis, N. Boucherit, S. Joriet, J. Wilimski, J. Electrochem. Soc. 137 (1990) 2684–2689.
[8] M. Stratmann, K. Bohnenkamp, H.–J. Engell, Corros. Sci. 23 (1983) 969–985.